Available online at www.eccomasproceedia.org
Eccomas Proceedia SMART (2023) 1535-1546

ECCOMAS
Proceedia

X ECCOMAS Thematic Conference on Smart Structures and Materials
SMART 2023
D.A. Saravanos, A. Benjeddou, N. Chrysochoidis and T. Theodosiou (Eds)

ELECTRONICS FOR PIEZOELECTRIC MEMS MICROPHONE ARRAYS APPLIED TO AERO-ACOUSTIC CHARACTERIZATION OF STRUCTURES IN WIND TUNNEL TESTS

CINDY A. BÁEZ, JOSÉ A. GARCÍA-SOUTO, PAULA CAVARISCHIA, AND PABLO ACEDO

Sensors and Instrumentation Techniques Group
Departamento de Tecnología Electrónica
Universidad Carlos III de Madrid
Leganés, Madrid, Spain
e-mail: cbaez@pa.uc3m.es, jsouto@ing.uc3m.es,
100406305@alumnos.uc3m.es, pag@ing.uc3m.es

Abstract. The electronic instrumentation system for a MEMS microphone array for wind tunnel tests (WTT) is presented: the array on a flexible PCB, the integration with the front-end electronics, the selection of components, the characterization of the electronics and the multiplexing strategy to concentrate analog channels in the data acquisition system (DAQ). This work is carried out in the framework of the Aeromic project, with new piezoelectric MEMS dual frequency LF (30 kHz resonance) and HF (200 kHz resonance) sensors.
The front-end and signal conditioning are based on commercial components, including integrated circuits for amplification and buffering, filtering, sample & hold, and multiplexing. The design and characterization of these electronic components are discussed. A modular design based on an 8-microphone array focuses on 4 analog channels of the DAQ through 8 analog multiplexers which is scalable to 80 sensors.

Key words: Instrumentation system, Sensor array, Harsh-environment, Wind tunnel tests, MEMS microphone, piezoelectric.

1 INTRODUCTION

The Aeromic project [1] aims to increase the environmental performance of aircraft by developing a sensing technology for aeroacoustics measurements with high spatial resolution (up to 2 mm), temporal resolution (1 µs), and a wide frequency range (up to 100 kHz). For this purpose, new dual-frequency piezoelectric MEMS sensors have been developed that provide with two AC-coupled outputs of different frequency range - lower frequency (LF) and higher frequency (HF) -, with dimensions of 900 µm x 1450 µm, and a dynamic range of 40 - 172 dB SPL [2]. These characteristics allow them to meet the CleanSky2 requirements for Wind Tunnel Tests (WTT) summarized in Table 1.

From the point of view of the sensitivity, piezoelectric MEMS sensors are a good alternative for acoustic measurements. For example, Lee et al. developed a piezoelectric transducer based on a multi-layer diaphragm fabricated by micromachining. It is a cantilever structure that serves both as a sensor (microphone) and actuator (loudspeaker) [3]. It has a

Peer-review under responsibility of the organizing committee of SMART 2023.
doi: 10.7712/150123.9925.446129

constant high sensitivity of 3 mV/µbar (30 mV/Pa) at low frequency and up to 20 mV/µbar (200 mV/Pa) at the first resonant frequency of 890 Hz.

Table 1: General requirements for aero-acoustic MEMS microphones in Wind Tunnel Tests (WTT)

Parameters	WTT Open	WTT Closed
Dynamic range [dB SPL]	0 – 140	30 – 150
(Airframe / Engine noises)	/ 30 – 170	/ 30 – 170
Bandwidth (±3 dB) [Hz]	100 – 35 k	100 – 100 k
SNR (ref. 120 dB SPL) [dB]	90	90
Temperature range [°C]	-50 – 70	-20 – 70
Ambient pressure [kPa]	99 – 102	99 – 102 / 500
Environment conditions	50% humidity /seeding particles	

Several custom MEMS microphones have been developed with aero-acoustic applications in mind and addressing the demands of sensitivity and dynamic range, despite the small size of their sensitive surface (½ inch or ¼ inch) that favors their integration [4,5]. Starting from multiple sensors with a dynamic range that allows measuring up to 155 dB with a noise level of 92 $dB \cdot Hz^{-1/2}$ [6], up to single samples that have reached more than 170 dB with a minimum detectable 40 dB [4].

While the most advanced surface-mounted MEMS microphones provide the necessary small size, sensitivity, and dynamic range, their bandwidth is in the range of consumer MEMS microphones: up to 20 kHz [6], limited to 6 kHz for those with higher dynamic range [4] or with a maximum of 10 kHz in multi-sensor arrays [7]. Aeromic's new dual-frequency piezoelectric MEMS microphones combine in each sensor two thin triangular structures similar in appearance, but different in size. They are an evolution from four identical isosceles triangular cantilevers, as developed for general-purpose piezoelectric MEMS microphones, to a design with asymmetrical scalene triangular cantilevers: two large ones covering the response in the low frequency range (up to 10 kHz, with 30 kHz resonance) and two small ones performing better at higher frequencies (up to 100 kHz, with 200 kHz resonance) [2,8]. This covers the entire bandwidth required for wind tunnel testing (Table 1).

From the perspective of the application with distributed sensors, Ahlefeldt et al. describe a thin array (thickness between 1.4 mm and 2.5 mm) of 45 MEMS microphones to measure pressure fluctuations on the airframe surface by performing analysis in the wavenumber domain. This MEMS solution is low cost and has better resolution compared to conventional microphones [6]. It uses MEMS microphones with analog output (ICS-40617) integrated on a flexible printed circuit board and connected to 45 channels of a data acquisition system (DAQ). Each microphone integrates the sensor, the impedance matching and the amplifier with differential output. It measures up to 132 dB SPL with -38 dBV sensitivity and frequency response from 50 Hz to 20 kHz resonance. The surface mount package has

dimensions of 3.50 mm x 2.65 mm x 0.98 mm [9]. Furthermore, an array of 256 MEMS microphones has even been successfully deployed for aero-acoustic measurements and used in open wind tunnel tests [7]. In this case the sensors are custom-made and grouped in arrays of 8 synchronized elements that are connected to a PC to measure up to 10 kHz. Also relevant to this paper is a previous work describing a first approach in the design of signal conditioning electronics for piezoelectric MEMS microphone arrays applied to aero-acoustic measurements, where the sensor signals are separated by frequency ranges and by measurement ranges [10].

In this paper we present, on the one hand, a compact preamplification stage implemented together with MEMS sensors to be integrated on a flexible PCB and adaptable to the shape of airframe samples. On the other hand, the design of the multi-stage amplification and two filter chains is presented. They provide frequency ranges from 100 Hz to 10 kHz and from 10 kHz to 100 kHz for the LF and HF sensor output, respectively. Additionally, the multiplexing stage is presented for the case of an array of 8 dual-frequency dual-range microphones, as well as its scalability for an array of 80 sensors. Finally, the characterization of noise and resolution, frequency response, linear distortion, and delay of the signal conditioning system are included.

2 INTEGRATION OF MEMS MICROPHONE ARRAYS

The sensors and the front-end conditioning are performed on flex printed circuits [11], and the amplification and filtering stages, along with the multiplexing stages of the signals, are performed on rigid PCBs (Fig. 1), so the integrated circuits (IC) chosen are optimized for size and versatility.

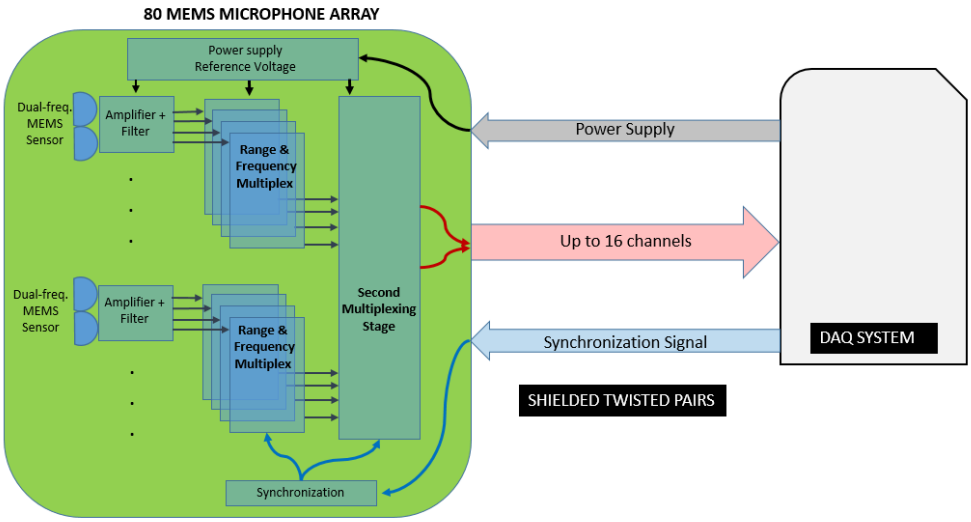

Figure 1: Block diagram of the conditioning system connected to the DAQ

The acquisition system is made with a modular controller, two 12-bit acquisition modules with 8 analog channels each working in the 6 V range. Considering a sensitivity of the sensor

of 5 mV/Pa, the expected voltage at full scale saturates each range of the electronics and the DAQ. On the other hand, the dynamic range is 140 dB. To cover the whole signal range from 30 dB SPL to 170 dB SPL, each section of the sensor (i.e. each frequency range) is conditioned through two chains with different gain/attenuation: the high-sensitivity chain that amplifies the sensor output and has a range up to 100 dB SPL (contributing to the least significant bits LSB), and the high-intensity chain that attenuates the sensor output and has a minimum detectable signal of 100 dB SPL (contributing to the most significant bits MSB). The amplification and attenuation are designed to handle the same voltage ranges at the DAQ input in both cases [10]. As a result, 4 signals (two frequencies and two ranges) are obtained from each sensor (Fig. 2).

A first approach of the front-end was thought to perform an amplification stage, so an operational amplifier with four channels for the four signals per sensor was used, meeting the noise and bandwidth specifications required for the application. However, due to the necessary simplification of the system to be integrated in the flex PCB, it was decided to incorporate only one amplifier in buffer mode for each frequency range, obtaining two signals per sensor. In this case, the amplification/attenuation chains are included in a second conditioning stage.

For the filtering stage, an integrated unit was chosen that allows up to four continuous-time second order low-pass and high-pass filters. To avoid multiple output cables, two analog multiplexing stages were added, the first one to multiplex 8 sensors into 4 outputs (per range and per frequency), and the second one to multiplex each of these categories resulting in 16 channels for 80 sensors.

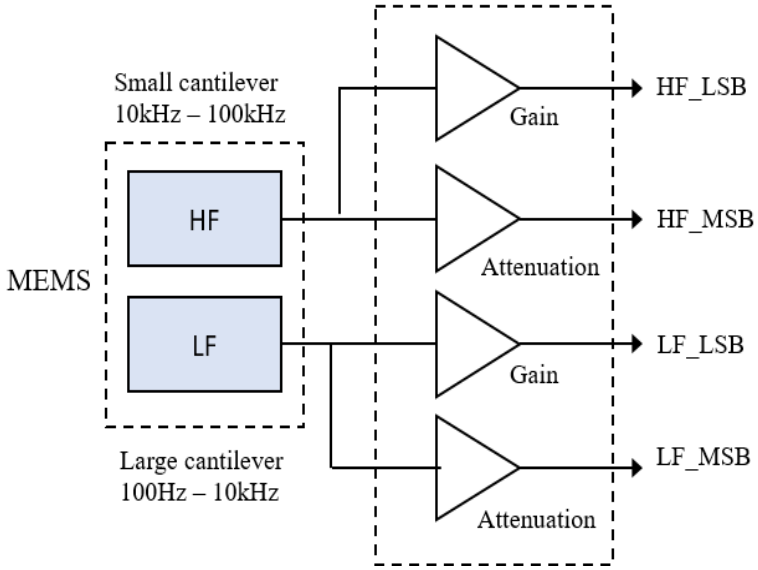

Figure 2: Amplification of each section of dual-frequency piezoelectric MEMS sensors

The array of 80 sensors has a specific distribution for the positioning of the sensors [6]. Considering the criteria of proximity to define the 8 most critical sensors [10], a 3D

approximation of the flex PCB design is performed, the first one with the amplification stage integrated with the sensors, and the second one with an amplifier in buffer configuration (Fig. 3). This second approach is performed with a 10-lead integrated circuit with LFCSP package (3mm x 3mm x 0,75 mm) that is more compact than the previous one. Additionally, it has a DIE version which is ideal for future developments, since in this case the signal conditioning and the sensor are integrated in a single package.

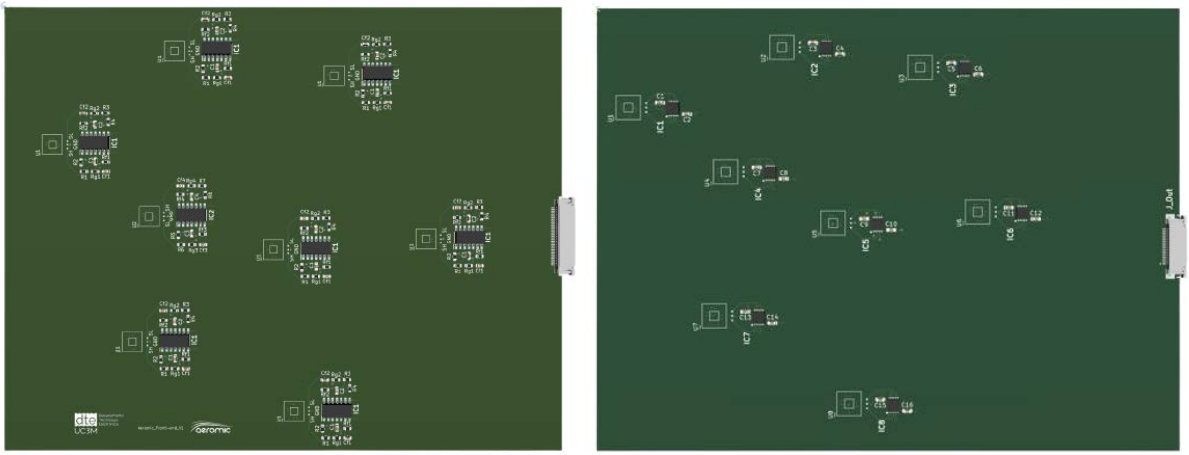

Figure 3: Examples of front-end for 8 sensors: With amplification (left); With buffering (right)

3 COMPONENTS SELECTION AND ELECTRONICS DESIGN

The selection of the components has been made considering the power supply ranges, bandwidth, noise, and the type of encapsulation of each integrated circuit as summarized in Table 2. It is established that the power supply for the whole conditioning system will be dual at ±5 V and will be provided by batteries.

Table 2: Characteristics of the integrated circuits

Characteristic	ADA4099-2	OP462	LTC1562	AD1608
Bandwidth [Hz]	8 MHz [0 dB]	15 MHz [0 dB]	10 kHz – 150 kHz	40 MHz
#Channels	2	4	4	8:1
Supply [V]	50 (±25)	12 (±6)	10 (±5)	16 (±8)
Package	10-Lead LFCSP / DIE	14-LeadSOIC	20-LeadSSOP	16-Lead TSSOP

The front-end design uses the ADA4099-2 with 10-Lead LFCSP package, the buffer configuration is set for both HF and LF frequency ranges, so at the output of the flex PCB we have the power supply up to ±25 V and two signals per sensor.

The amplification stage is performed for each frequency section of the sensor. A basic dynamic range (LSB) uses 2 x 15 V/V amplification to satisfy the minimum detectable signal with the resolution of the analog inputs of the DAQ, and an extended dynamic range (MSB)

with 1/15 V/V attenuation satisfies a sound level of 170 dB SPL (Table 3). In the LSB range, the voltage-mode amplifier model [12] was used (Fig 4). Given the high-pass effect of the sensor, a parallel resistor is set to control the cut-off frequency. For the MSB range, a voltage divider with two resistors attenuates the signal to minimize the linear distortion.

Table 3: Amplifier ranges and stages

Input Dynamic Range [dB SPL]	Sensor Output Dynamic Range [Vrms]	Amplification (1st Stage) [V/V]	Amplification (2nd Stage) [V/V]
LSB 30 – 100	3.16 µV – 10 mV	15	15
MSB 100 - 170	10 mV – 31.62 V	1/15	1

The filtering stage was performed with the LTC1562 integrated circuit that has several configurations controlled through external components for several types of filters. To optimize the number of components on the PCB, it was decided to implement 4 second order filters on each IC. The design requires low pass filters (LPF) with cut-off frequencies of 10 kHz for the LF range and 100 kHz for the HF range. In addition, high pass filters (HPF) with a cut-off frequency of 10 kHz are implemented for the HF range. In the case of LF, the high pass behavior is given by the sensor.

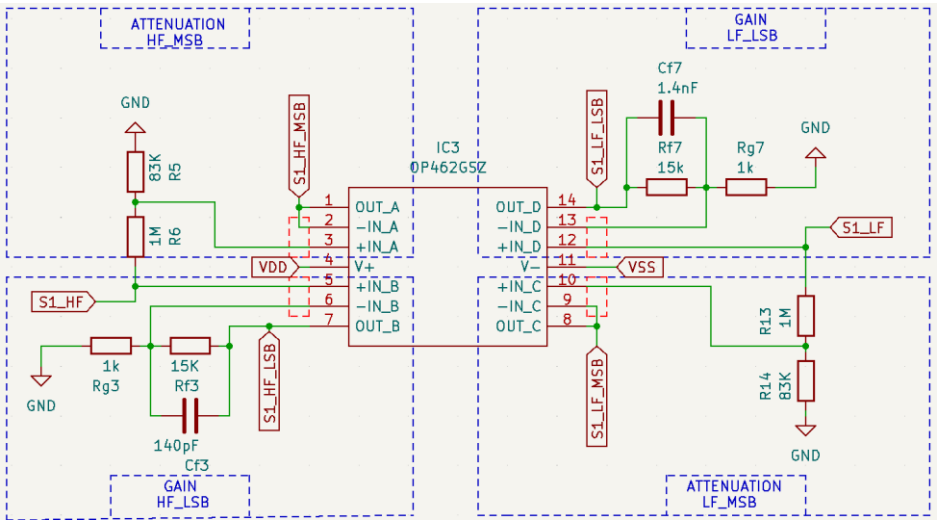

Figure 4: Amplification stage circuit for two frequency ranges and two signal amplitude ranges

The multiplexing stage is based on the AD1608 integrated circuit. The stage requires a minimum sampling frequency that is bound by the HF frequency range (10 kHz -100 kHz). To meet the Nyquist criterium, the sampling frequency is set at 200 kHz, so the clock input to the time multiplexing of 8 sensors is 1.6 MHz. To avoid loss of information, a sample and hold (S&H) stage is implemented with the AD783 integrated circuit which provides with 200 ns of transition time and 0.02 µV/µs of drop rate. The AD783 provides the S&H of a single

sensor channel. The synchronization of both stages is done by the clock signal that is connected to an input channel of the DAQ.

The second stage of multiplexing is to scale the matrix from 8 sensors to 80, so a multiplexing is performed for each category of the signal (ranges and frequencies), using 4:1 multiplexer for LF channels and 2:1 multiplexer for HF channels, resulting in 16 outputs that are connected to the DAQ channels. The sampling frequency of the second stage is 3.2 MHz, which produces a decimation of the LF channels to 100 kSps, but enough for the 10 kHz bandwidth. The demultiplexing is performed by software in the DAQ system (1x16 and 1x32).

The amplification and filtering stages are placed on a PCB (Fig. 5). The input of this conditioning system is the flex PCB with the sensor array and the front-end (Fig. 3), and the output is connected to the next multiplexing stage.

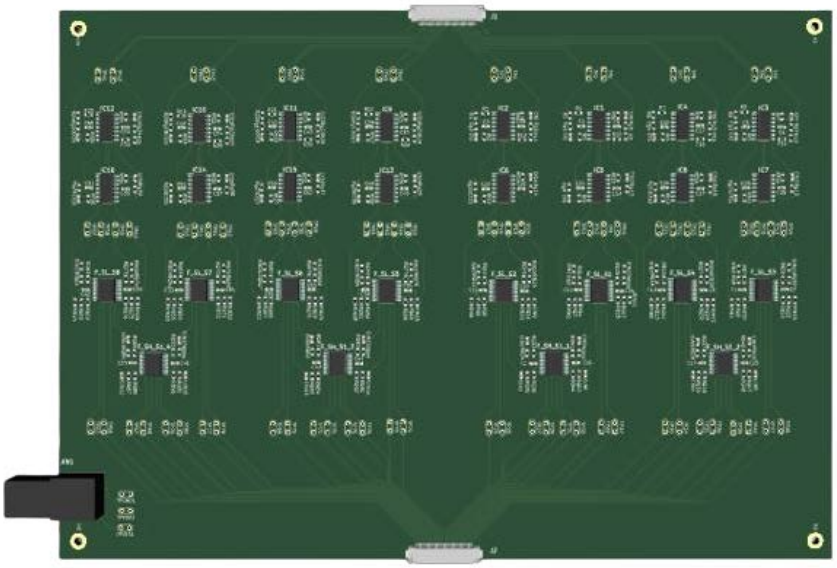

Figure 5: Conditioning and filtering of 8 microphones

The acquisition system is based on a PXIe-8135 controller programmed in LabVIEW 2019, using two PXI 5105 modules with 8 analog channels each one and a PFI1 channel for the trigger function. The sampling frequency is > 3.2 MHz, and oversampling is available up to 18. The system saves files identified by module, sensor, frequency, and range that can be stored directly on an external disk without loss of information in 2 s continuous monitoring frames.

4 ELECTRONICS CHARACTERIZATION

The different types of channels have been characterized to obtain the noise and resolution, sensitivity and frequency response, harmonic range and distortion, and inter-channel delay.

The actual noise characterization was performed using a lock-in amplifier (HF2, Zurich Instruments). The input of the conditioning system was connected to ground and the output

was connected to the HF2. We performed a sweep in a specified frequency range (10 Hz – 1 MHz) with a selection of the number of points equal to 1000.

The results obtained from the characterization (Table 4) are within the estimated range and do not exceed the noise limits of the project specifications. Note that, although the noise of MSB channels is in the range of 100 dB SPL, the minimum detectable signal and the signal to noise ratio are satisfied by the LSB channels. Fig. 6 shows the simulated noise referred to the output of a HF channel with a characteristic band-pass between 10 kHz and 100 kHz.

Table 4: Noise characterization measurements

Characteristic	LF_LSB	LF_MSB	HF_LSB	HF_MSB
Gain [V/V]	225	1/15	225	1/15
Sensitivity [dB re 1 V/Pa]	61	-69.5	61	-69.5
Noise Bandwidth [Hz]	100 - 10k	100 - 10k	10k - 100k	10k - 100k
$^{(1)}$ $_{TO}$ **[µVrms]**	34.5	14.3	26.3	73.4
$^{(2)}$ $_{TI}$ **[µVrms]**	0.15	214	0.12	1101
Noise Equivalent Pressure [dB SPL]	29.7	92.6	27.4	106.9

$^{(1)}$ $_{O}$ Noise referred to the output of the filtering stage. $^{(2)}$ $_{I}$ Noise referred to the input of the amplifier.

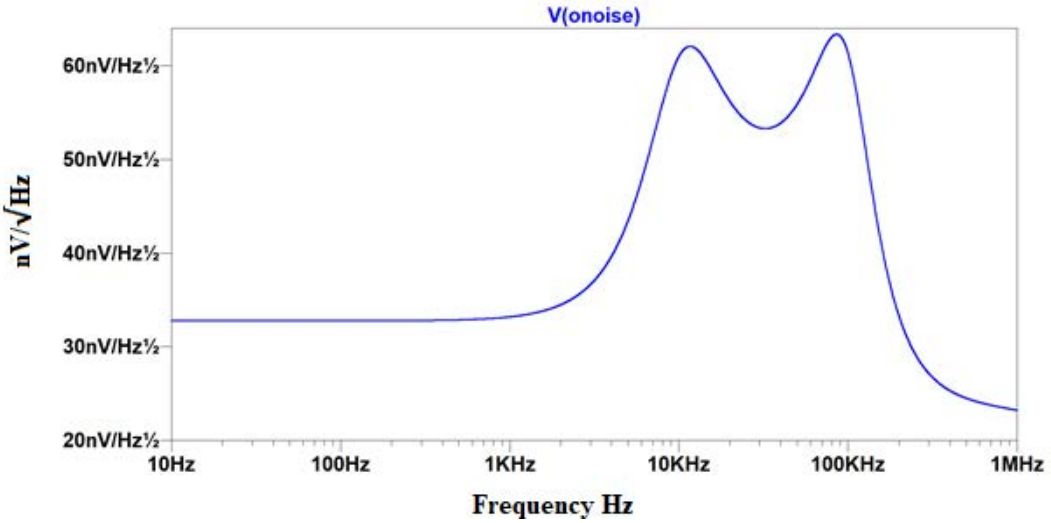

Figure 6: Noise characterization: Simulated output HF_MSB

The frequency characterization was performed with pure tones using a signal generator source. A signal of 10 mV peak to peak was generated for the LSB range, and 1 V peak to peak was generated for the MSB range. Compared to the simulation, the results obtained at

the amplifiers outputs are as expected: the signal in the MSB range is attenuated by a factor of 15 V/V, and the LSB range is amplified by a factor of 225 V/V.

In addition, the characterization was divided for each frequency and voltage range considered in the system. Figure 7 shows the simulation of the LF low-pass filtering for LSB range and MSB range.

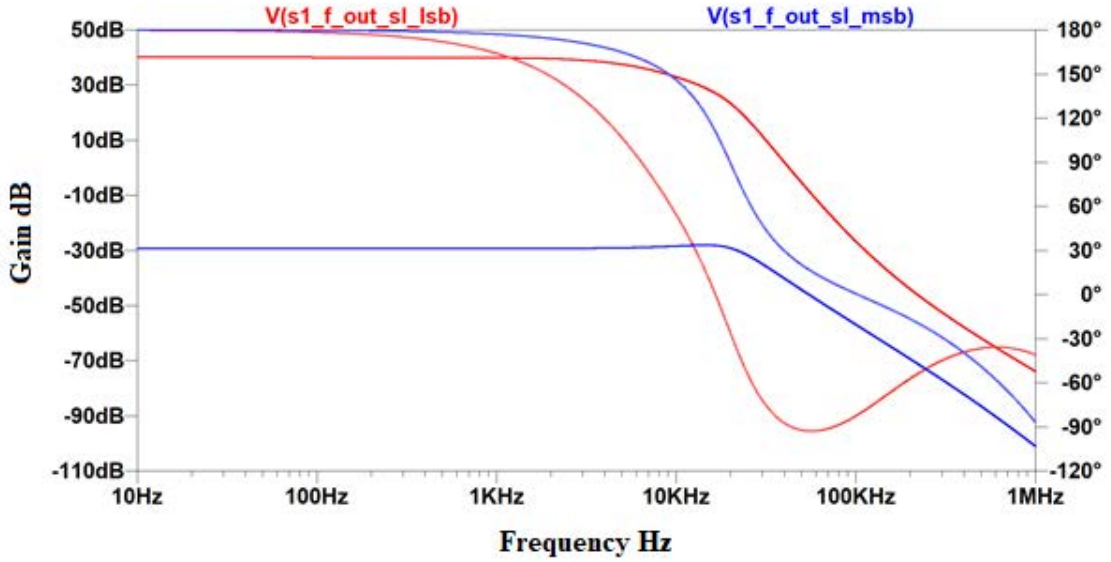

Figure 7: Simulated frequency response: Low-pass filtering of LF sections LSB and MSB

The measurement results of the system in Fig. 5 are summarized in Tables 5 and 6, for HF sections (bandpass from 10 kHz to 100 kHz), and for LF sections (lowpass up to 10 kHz), respectively. At the output of the filters, the signal is attenuated by a factor of between 2 dB and 10 dB, depending on the chain. The frequency response roll-off is mainly due to the second order filters (40 dB/decade); the bandwidth of each amplifier is at least one order of magnitude wider than the filters cut-off frequencies.

Table 5. Frequency response for HF (sensing 10 kHz – 100 kHz)

HF - MSB								
Frequency [kHz]	1	9	10	20	50	100	126	1000
Gain [dB]	-41	-36	-32	-33	-32	-35	-38	-41
HF - LSB								
Frequency [kHz]	1	8	10	20	50	100	131	1000
Gain [dB]	3	15	44	45	45	45	15	2

Table 6. Frequency response for LF (sensing 100 Hz – 10 kHz)

LF - MSB						
Frequency [kHz]	1	2	5	10	24	100
Gain [dB]	-25.5	-26.4	-26.3	-27.3	-29.4	-39.0
LF - LSB						
Frequency [kHz]	1	2	5	10	26	100
Gain [dB]	40.2	40.5	40.3	41.1	38.1	14.0

The characterization of the linear distortion was performed in the same way, using a signal generator source with pure tones of 1 kHz and 20 kHz. A signal of 27 mV peak to peak was generated for the LSB range, and a signal of 90 V peak to peak was simulated for the MSB range. In both cases, the output is adjusted to the DAQ input range, but it is a 60 % of the dynamic range given by the voltage supply of ±5 V. The effect of the sensor impedance on the amplifier distortion was not considered. The Fast Fourier Transform (FFT) was plotted, and the voltage values of both, the fundamental frequency, and the harmonics, were taken. Then, the linear distortion was calculated as a percentage with the root square of the sum of the squares of the harmonic voltages divided by the voltage of the fundamental frequency.

The characterization of the system delay is performed at the output of the filters stage. A square signal, 1 kHz repetition rate, is introduced to the system inputs. It is expected the delay in all channels to be systematic, and a maximum difference of 1 μs among channels is specified for the application. The critical contribution is from the time multiplexing. In order to reduce it, a synchronization of the multiplexed channels is provided by the sample & hold circuits. The low tolerance of the AD783 time response (0.01%) allows us to minimize the differences between channels. The low-rate voltage drop in the holding circuit (20 nV/μs) has no impact on the accuracy for periods of 5 μs between samples (200 kHz). The inter-sensor delay does not exceed 1 μs and the only impact is on the synchronization of different types of channels.

5 DISCUSSION

The design is based on a first approximation of the Aeromic Project sensors with a sensitivity of 5 mV/Pa. However, for the new sensors it is sufficient to modify the values of the amplifier stage components, since the actual bandwidth of the amplifiers exceeds the requirements.

The LTC1562 filters were chosen due to their versatility to implement 4 filters in a single integrated circuit. However, being 10 kHz the limit of its established bandwidth, it is necessary to implement 1 MΩ resistors, which increases the noise, and a resonant frequency response is obtained. To compensate for this effect, the low pass filter (LPF) was designed for the LF frequency range (100 Hz – 10 kHz) with a cut-off frequency of 14.65 kHz. The high-

pass effect given by the piezoelectric sensor is compensated by a shunt resistor, so we can control the lower cut-off frequency of the system.

There is a variety of commercial integrated circuits, those that have been implemented were chosen for their versatility, considering that they meet the specifications of the project. The implemented amplifier (OP462) has a noise voltage of 33 nV/√Hz. There are other amplifiers specifically designed for low noise, such as the ADA40992 with a noise voltage of 7 nV/√Hz, and 2 channels, but 4 channels are needed to cover all ranges. The AD8429, with a noise voltage of 4 nV/√Hz, has been considered for future designs.

The challenge of this signal conditioning system design was to support the acquisition of 80 dual sensors with 24-bit resolution to cover the 140 dB dynamic range, and the frequencies 100 Hz - 10 kHz for LF range and 10 kHz - 100 kHz for HF range, with low noise electronics.

This was achieved by using a 16-channel acquisition system with 12-bit resolution, and by dividing the range for strong and weak signals, with two amplification stages for the LSB signals and one attenuation stage for the MSB range. This means that, instead of 80 sensors, we have 320 signals (4 per sensor), and only 16 channels. This was solved by designing two multiplexing stages, the first one with 8:1 multiplexers to concentrate the signals from each sensor by range and frequency, and the second one to concentrate all these signals into 15 channels using 4:1 and 2:1 multiplexers, depending on their range and frequency, and leaving one channel for the synchronization signal.

6 CONCLUSIONS

The design and characterization of the electronics for a MEMS microphone array were discussed. The specifications for wind tunnel tests have been considered. The electronics designed for 8 sensors is scalable to 80 sensors for the final array of the Aeromic project.

To avoid signal loss or overflow in the acquisition system, the input range is divided into LSB (30 dB SPL – 100 dB SPL) and MSB (100 dB SPL – 170 dB SPL), which allows us to amplify the weak signals and attenuate the strong signals to handle a single acquisition input range. In addition, two-sections piezoelectric MEMS transducers provide two ranges of frequency (LF 100 Hz – 10 kHz and HF 10 kHz – 100 kHz). The hardware multiplexing of the four sections per sensor and the sensor array is demultiplexed by software in the DAQ.

The results of the system characterizations verify that the electronics meet the specifications imposed in the project. However, with the sensor sensitivity set at 5 mV/Pa, it is verified that the measurement of noise introduced by the sensor is the predominant one in the system.

The acquisition system with a sampling frequency of 60 MSps allows us to oversample the signals, thus avoiding the loss of information and facilitating the reconstruction of the signals after demultiplexing.

7 AKNOWLEDGEMENTS

This project has received funding from the Clean Sky 2 Joint Undertaking (JU) under grant agreement No 101007958. The JU receives support from the European Union’s Horizon 2020

research and innovation program and the Clean Sky 2 JU members other than the Union.

REFERENCES

[1] "AEROMIC," 2020. Available: https://aeromic-cleansky.eu/.

[2] L. Wu, M. Moridi, G. Wang y Q. Zhou, "Microfabrication and characterization of dual-frequency piezoelectric micromachined ultrasonic transducers," 2021 IEEE International Symposium on Applications of Ferroelectrics (ISAF), Sydney, Australia, 2021, pp. 1- 4.

[3] Seung S. Lee, R. P. Ried y R. M. White, "Piezoelectric cantilever microphone and microspeaker," in Journal of Microelectromechanical Systems, vol. 5, no. 4, pp. 238-242, Dec. 1996.

[4] M. D. Williams, B. A. Griffin, T. N. Reagan, J. R. Underbrink, and M. Sheplak, "An AlN MEMS Piezoelectric Microphone for Aeroacoustic Applications," Journal of Microelectromechanical Systems, vol. 21, no. 2, pp. 270-283, April 2012.

[5] R. Littrell and K. Grosh, "CModeling and Characterization of Cantilever-Based MEMS Piezoelectric Sensors and Actuators," Journal of Microelectromechanical Systems, vol. 21, nº 2, pp. 406-413, April 2012.

[6] T. Ahlefeldt, S. Haxter, C. Spehr, D. Ernst y T. Kleindienst, "Road to Acquisition: Preparing a MEMS Microphone Array for Measurement of Fuselage Surface Pressure Fluctuations," Micromachines, vol. 12, no. 8, p. 961, Aug. 2021.

[7] Y. Zhou, V. Valeau, J, Marchal, F. Ollivier and R. Marchiano, "Three- dimensional identification of flow-induced noise sources with a tunnel- shaped array of MEMS microphones," J. Sound Vib, vol. 482, 115459, 2020.

[8] L. Wu, X. Chen, H. D. Ngo, E. Julliard, and C. Spehr, "Design of dual- frequency piezoelectric MEMS microphones for wind tunnel testing," in AIAA Advanced Testing and Measurement Techniques, 2021, no. 1021.

[9] J. Karki, Texas Instruments, "Signal Conditioning Piezoelectric Sensors," Application Report SLOA033A - September 2000.

[10] J. A. García-Souto, J. Lázaro-Fernández and Pablo Acedo, "Signal conditioning design for aero-acoustic piezoelectric MEMS microphone arrays," 2022 Symposium on Design, Test, Integration and Packaging of MEMS/MOEMS (DTIP), Pont-a-Mousson, France, 2022, pp. 1-4.

[11] K. Erbacher, J.A. Marques, M. von Krshiwoblozki, L. Wu, H. D. Ngo, and M. Schneider-Ramelow, "Aero Acoustic MEMS Microphone Integration in Ultra-Thin and Flexible Substrate," 2022 IEEE 24th Electronics Packaging Technology Conference (EPTC), Singapore, Singapore, 2022, pp. 15-18.

[12] ICS-40618 Datasheet. DS-000044-ICS-40618-v1.0.pdf. https://invensense.tdk.com